Mathematical & Computational Applications, Vol. 8, No. 1 , pp. 1-11, 2003

EFFECT OF SHAFT ELASTICITY ON THE PERFORMANCE OF SLIP ENERGY RECOVERY DRIVES

Salwa Saleh Basurrah Mehmet Akbaba
Department of Electrical and Electronics Engineering, College of Engineering
University of Bahrain, P.O. Box 33547, Isa Town, State of Bahrain
akbaba@eng.uob.bh or akbaba@batelco.com.bh

Abstract- All rotating shafts, even in the absence of external load, deflect during rotation. The magnitude of the deflection depends upon the stiffness of the shaft, its supports and also upon the load level. In this paper, a complete study of the effect of shaft elasticity or stiffness coefficient on the performance of a slip energy recovery drive (SERD) has been presented. The elastic shaft model is derived through the use of Lagrange formulation and it is incorporated into the slip SERD model. A computer program is developed to analyze the complete performance of the drive including the effect of shaft elasticity. A load torque that is a quadratic function of the shaft speed is assumed throughout the analysis. Numerous computer simulations were carried out to illustrate the performance of the SERD with elastic transmission for different stiffness coefficients of the shaft material, taking into account the effects of changing the modulus of elasticity and shaft dimensions.
Keywords- Slip energy, elastic shaft, Lagrangian, performance, SERD

1. INTRODUCTION

The deflection of the rotating shafts is a function of speed, and they show some maximum values at so-called critical speeds. For any shaft there are an infinite number of critical speeds, but only the lowest (first) and occasionally the second are generally of interest to the designers. The others will usually be so high as to be well out of the range of operating speeds. The shafts are classified according to the first critical speed. A flexible shaft is the one which operates close to, or beyond its first bending critical speed, for dynamic effects to influence the shaft deformations. On the other hand a shaft which operates substantially below its first bending critical speed is considered to be a rigid shaft. Those shafts that are made of materials with higher Young's modulus, E, are regarded as rigid ones[1].

From material stand point, if the same materials are used for either type of design i.e. elastic or rigid; then the geometry of the shaft will have effect on the stiffness of the shaft. The greater the stiffness of the shaft the less it will twist for a given torque transmitted through the shaft. As consequence, it is important to distinguish between material properties and design properties because they may be varied independently. We may define a stiff material as one with a high value of E, whereas a stiff design is one with a high value of second moment of area of the cross section, J_r, i.e. a dimension of the shaft.

For electric motors designs, shafts are designed as flexible such that the operating speed is at least 10% higher than the critical speed [2]. So the shaft is only at critical speed where it flexes for a short time when coming up from standstill to operating speed or coasting to a stop. This is why these types of shafts are acceptable to the user since the shaft is flexing only for a few seconds while the shaft speed passes through

the critical frequency. This gives opportunity to use less material and hence reduce the capital cost of the shaft and of the machine as overall. Shaft designs having long length with small diameter are cheaper than that of large diameter and short length. That is because the cost is directly proportional to $D^2_{shaft} \times L_{shaft}$, i.e., cost goes up in proportion to the square of the diameter.

Elastic shafts are popular today because as it is mentioned previously, their use will allow the designer to design a smaller machine thus saving money. They are usually used for induction motors of large horsepower i.e. greater than 300HP and two pole machines [3].

Some recent research efforts have been devoted to considering the effect of elastic transmission on the performance of electric drive systems [4,5]. The behavior of a speed control system for electrical drives with elastic transmission were analyzed [4] taking a constant stiffness coefficient to represent the elasticity of the shaft. Analysis of a speed control system for electrical drives with elastic transmission based on Bode method is described in [5]. However, in previous investigations the effect of elastic shafts on the performance of the SERD did not receive any attention.

In this paper, therefore, the effect of flexible shafts on the performance of the SERD will be studied in details. Following the mathematical model of SERD, the behavior of elastic shafts will be modeled using Lagrangian formulation and finally it will be incorporated into the SERD model. The total system behavior will be demonstrated numerically using MATLAB [6].

2. MATHEMATICAL MODEL OF SERD

Figure 1 shows a schematic of a slip energy recovery drive. A slip-ring induction motor is connected to a three-phase uncontrolled rectifier, which is cascaded to a line-commutated inverter via a smoothing reactor. The AC side of the inverter is fed back to the supply through a step up transformer.

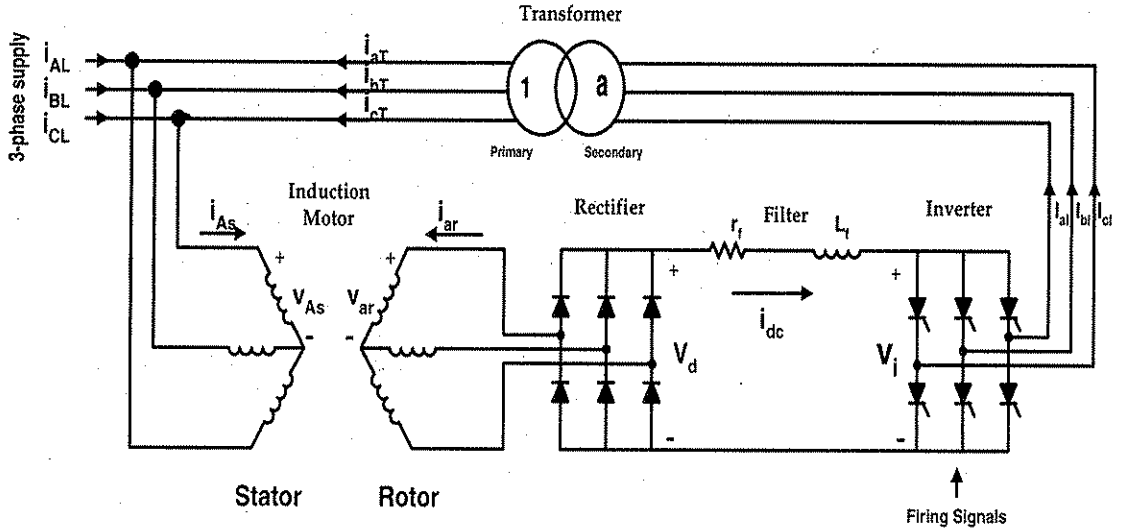

Figure 1. Schematic representation of a slip energy recovery system

The drive has been simulated using the hybrid dq-abc model as follows [7,8]:

$$\begin{bmatrix} v'_{ds} \\ v'_{qs} \\ v_{ar} \\ v_{br} \\ v_{cr} \end{bmatrix} = \begin{bmatrix} R_s + L_s p & -\omega_e L_s & Mp & \frac{-\left(Mp+\sqrt{3}M\omega_e\right)}{2} & \frac{\left(-Mp+\sqrt{3}M\omega_e\right)}{2} \\ \omega_e L_s & R_s + L_s p & M\omega_e & \frac{\left(\sqrt{3}Mp-M\omega_e\right)}{2} & \frac{-\left(\sqrt{3}Mp+M\omega_e\right)}{2} \\ Mp & 0 & R_r + \overline{L}_r p & \overline{M}_r p & \overline{M}_r p \\ -\frac{M}{2}p & \frac{\sqrt{3}}{2}Mp & \overline{M}_r p & R_r + \overline{L}_r p & \overline{M}_r p \\ -\frac{M}{2}p & -\frac{\sqrt{3}}{2}Mp & \overline{M}_r p & \overline{M}_r p & R_r + \overline{L}_r p \end{bmatrix} \cdot \begin{bmatrix} i'_{ds} \\ i'_{qs} \\ i_{ar} \\ i_{br} \\ i_{cr} \end{bmatrix} \tag{1}$$

where;

$$p\theta = \frac{d}{dt}\theta = \omega_e \tag{2}$$

$$\begin{bmatrix} v'_{ds} \\ v'_{qs} \end{bmatrix} = \begin{bmatrix} \frac{\sqrt{3}}{\sqrt{2}} V_m \cos(\omega_s t - \theta) \\ \frac{\sqrt{3}}{\sqrt{2}} V_m \sin(\omega_s t - \theta) \end{bmatrix} \tag{3}$$

where $i'_{ds}, i'_{qs}, i_{ar}, i_{br}, i_{cr}, v'_{ds}, v'_{qs}, v_{ar}, v_{br}, v_{cr}$ are the stator and rotor currents and voltages in 'hybrid' reference frame, respectively.

The electromagnetic torque can be obtained for the induction machine in 'hybrid' reference frame as given below;

$$T_e = \frac{P}{2}\left(\frac{\sqrt{3}}{2} i'_{ds} \cdot M \cdot \left(i_{cr} - i_{br}\right) - \frac{1}{2} i'_{qs} \cdot M \cdot \left(i_{cr} + i_{br} - 2i_{ar}\right)\right) \tag{4}$$

From the equation of motion one can write:

$$\frac{d\omega_e}{dt} = \frac{1}{J} \cdot \left(\frac{P}{2}\right) \cdot \left[T_e - B \cdot \left(\frac{2}{P}\right) \cdot \omega_e - T_L\right] \tag{5}$$

where T_L is the load torque, J is the moment of inertia and B is the coefficient of friction.

The three-phase uncontrolled rectifier is modeled assuming an overlap angle less than $\pi/3$ as in [8] with twelve conduction states based on the rotor slip-ring terminal voltages and currents. The three-phase bridge inverter is modeled and examined based on the theory presented in [7]. It is assumed that the ac supply and step down transformer have negligible commutating reactance.

3. MATHEMATICAL MODEL OF THE ELASTIC SHAFT

The calculus of variations provides an alternative characteristic of the motion of mass particles in the form of Hamilton's principle. Often the variational characterization is actually more effective for determining the motion of a dynamic system [9]. The derivation of the equations of motion can be obtained from variational principles applied to energy functions. There are a number of different energy functions (e.g. the Lagrangian, the total energy), which can be used as an energy

function. In this paper modeling of the shaft motion is mainly based on the Lagrangian that is a function of the generalized coordinates (non-Cartesian) and the associated velocities [10].

The motor, shaft and load system shown in Figure 2. The motor has inertia constant J_M and it generates electromagnetic torque of T_e. The load has inertia constant of J_L and a load torque T_L. The load is coupled to the motor through an elastic shaft with stiffness coefficient K.

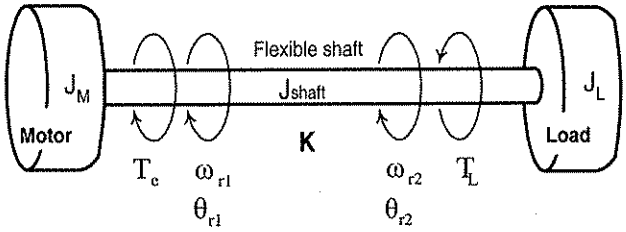

Figure 2. Motor-load drive system with flexible shaft

The geometric configuration of the system is determined completely by the generalized coordinates θ_{r1} and θ_{r2}, i.e., the rotational angles at the two ends of the flexible shaft and their associated angular velocities are ω_{r1} and ω_{r2}. The kinetic energy of the drive system is given by:

$$K_e = \frac{1}{2} J_M \cdot \omega_{r1}^2 + \frac{1}{2} J_L \cdot \omega_{r2}^2 \tag{6}$$

Next, the potential energy is given as:

$$P_e = \frac{1}{2} K (\theta_{r1} - \theta_{r2})^2 \tag{7}$$

where the stiffness coefficient K is given by [11]:

$$K = \frac{G_o \cdot J_r}{L_{shaft}} \tag{8}$$

where G_o is the shear modulus, J_r is the moment of inertia and L_{shaft} is the length of the shaft .

The Lagrange equations of motion for a non-conservative mechanical system is given by [10]:

$$\frac{d}{dt}\frac{\partial L_{ag}}{\partial \dot{q}_j} - \frac{\partial L_{ag}}{\partial q_j} = Q_j^e, \qquad j = 1, \cdots, n \tag{9}$$

where L_{ag} is the Lagrangian and are Q_j^e the generalized forces, q_j's are generalized coordinates. In our system we have two generalized coordinates, i.e., $q_1 = \theta_{r1}$ and $q_2 = \theta_{r2}$.

Therefore, Lagrangian follows as:

$$L_{ag} = K_e - P_e = \frac{1}{2} J_M \omega_{r1}^2 + \frac{1}{2} J_L \omega_{r2}^2 - \frac{1}{2} K (\theta_{r1} - \theta_{r2})^2 \tag{10}$$

The generalized forces are:

$$Q^e_{j=2} = [T_e \quad -T_L] \tag{11}$$

hence, $Q^e_1 = T_e$, $\quad Q^e_2 = -T_L$

In order to find the Lagrange equations of motions, at the two ends of the flexible shaft, we need to find:

$\frac{\partial L_{ag}}{\partial \theta_{r1}}, \frac{\partial L_{ag}}{\partial \theta_{r2}}, \frac{d}{dt}\left(\frac{\partial L_{ag}}{\partial \dot{\theta}_{r1}}\right)$ and $\frac{d}{dt}\left(\frac{\partial L_{ag}}{\partial \dot{\theta}_{r2}}\right)$, which are as follows:

$$\frac{\partial L_{ag}}{\partial \theta_{r1}} = -K \cdot (\theta_{r1} - \theta_{r2}) \tag{12}$$

$$\frac{\partial L_{ag}}{\partial \theta_{r2}} = K \cdot (\theta_{r1} - \theta_{r2}) \tag{13}$$

$$\frac{\partial L_{ag}}{\partial \dot{\theta}_{r1}} = \frac{\partial L_{ag}}{\partial \omega_{r1}} = J_M \cdot \omega_{r1} \tag{14}$$

$$\frac{\partial L_{ag}}{\partial \dot{\theta}_{r2}} = \frac{\partial L_{ag}}{\partial \omega_{r2}} = J_L \cdot \omega_{r2} \tag{15}$$

$$\frac{d}{dt}\left(\frac{\partial L_{ag}}{\dot{\theta}_{r1}}\right) = J_M \cdot \frac{d\omega_{r1}}{dt} \tag{16}$$

$$\frac{d}{dt}\left(\frac{\partial L_{ag}}{\partial \dot{\theta}_{r2}}\right) = J_L \cdot \frac{d\omega_{r2}}{dt} \tag{17}$$

Substituting of Equations (14), (15), (16) and (17) into Equation (9) leads to the following equations of motion:

$$J_M \frac{d\omega_{r1}}{dt} + K \cdot (\theta_{r1} - \theta_{r2}) = T_e \tag{18}$$

$$J_L \frac{d\omega_{r2}}{dt} - K \cdot (\theta_{r1} - \theta_{r2}) = -T_L \tag{19}$$

By arranging the above two equations; the following four equations will be found:

$$\frac{d\omega_{r1}}{dt} = \frac{1}{J_M}[T_e - K \cdot (\theta_{r1} - \theta_{r2})] \tag{20}$$

$$\frac{d\omega_{r2}}{dt} = \frac{1}{J_L}[K \cdot (\theta_{r1} - \theta_{r2}) - T_L] \tag{21}$$

$$\frac{d\theta_{r1}}{dt} = \omega_{r1} \tag{22}$$

$$\frac{d\theta_{r2}}{dt} = \omega_{r2} \tag{23}$$

Equations (20),(21), (22) and (23) represent the mathematical model of the elastic shaft and these four equations will replace equation of $d\omega_e/dt$ that appears in the hybrid model for each of the six rectifier conduction states that are given in [8].

4. APPLICATION EXAMPLE

A 7.5KW, 415V, 14.2A, 50Hz, 4 pole slip-ring induction motor coupled to slip energy recovery rectifier, inverter and transformer has been taken as application example. The motor parameters which all are referred to stator side are as follows:

$R_s = 0.143\,\Omega \quad L_s = 0.0371\,H \quad R_r = 0.191\,\Omega \quad L_r = 0.0371\,H \quad M = 0.0288\,H$

DC link reactor has parameters as:

$$R_f = 0.2\,\Omega \qquad L_f = 0.039\,H$$

The recovery transformer has turns ratio of $a = 0.59$ and magnetizing reactance of X_M=179Ω and the thyristors that are used in the recovery inverter are having holding current of I_h=0.5A.

A simulation computer program has been prepared to simulate the system described in sections 2 and 3. The full performance of the drive has been demonstrated. In order to investigate clearly the effect of flexible shaft, the performance of SERD is computed for several values of stiffness coefficient and results are compared in the following sections.

The slip-ring induction motor with a flexible shaft model has been started through a three phase bank of external resistors and run up until equal speeds of 109.8 rad/sec are reached at the both ends of the shaft, i.e., full equilibrium is reached at steady-state operation. The load torque connected to the induction motor via the flexible shaft is given by:

$$T_L = k_1 \cdot \omega_{r2} + k_2 \cdot (\omega_{r2})^2 \qquad (24)$$

where values of the load torque coefficients are:

$k_1 = 0.04$ Nm/rad/sec and $k_2 = 0.0023$ Nm/(rad/sec)^2

After reaching the steady-state speed, the slip energy recovery system has been connected by switching rotor terminals from resistor bank to recovery rectifier. The inverter-firing angle has been adjusted to a value of 101°.

To study the effect of different stiffness coefficient, K, the performance of the drive system is calculated for three different values of K, i.e., K=450Nm/rad, K=297Nm/rad and K=45Nm/rad and the results are compared in Figs.3 to 7.

From Fig.3.a it is clearly seen that with a stiffness coefficient K= 450Nm/rad, which is considered to be a high value at which the shaft performs almost as a rigid one, the angle difference at the shaft endpoints starts with a small value and once it is connected to the recovery circuitry, it oscillates until it reaches the steady-state. At steady-state the amplitude of the oscillations attenuates to a very small value with an average of 0.077 radians (almost 4.4 degrees). It is obvious that the value of the angle from the motor side θ_{r1}, is always having values greater than the angle from the load side θ_{r2}, which is expected to be so.

Further decrease in the value of the stiffness coefficient, K=297Nm/rad, will increase the difference between the angular displacements on both shaft ends. This is shown in Fig.3.b. It is clear that the starting transients have been increased in magnitude compared to Fig.3.a, and as it reaches the steady-state, the oscillations will have smaller deviation from an average of 0.117 radians (about 6.7°).

It is clearly seen from Fig.3.c that with further reduction of K, which means more flexible shaft, smooth oscillations takes place during transient period but the amplitude

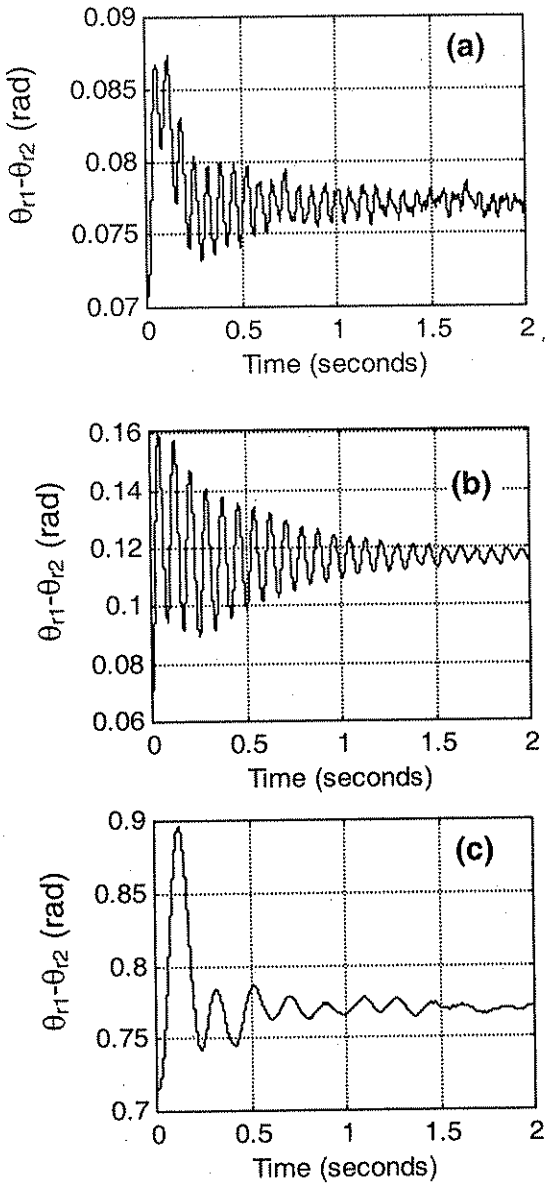

Figure 3. Difference of the mechanical angles on both endpoints of the shaft.
a) K=450 b) K=297 c) K=45

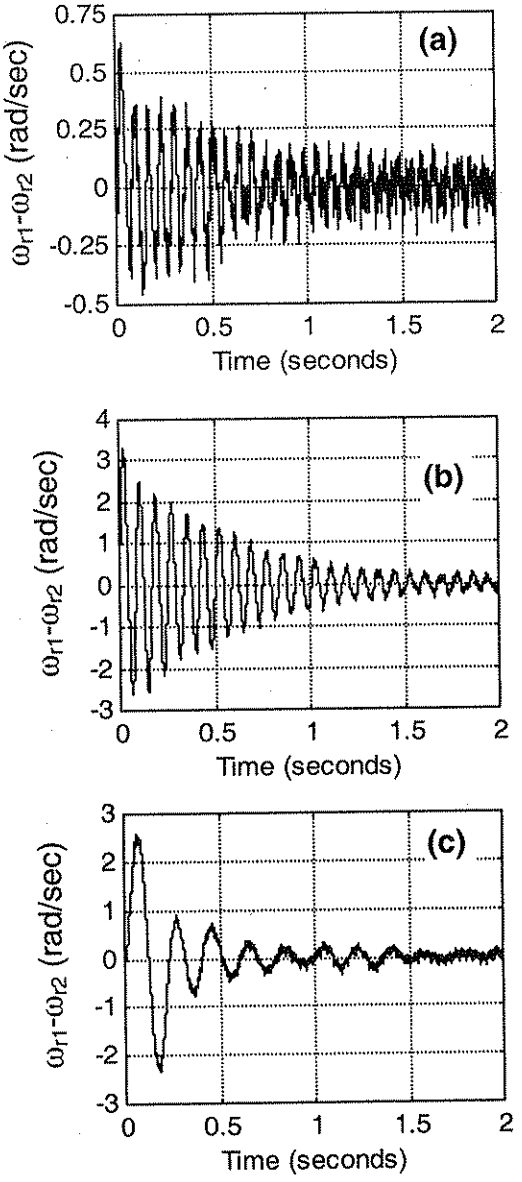

Figure 4. Difference of the mechanical speeds on both endpoints of the shaft.
a) K=450 b) K=297 c) K=45

of the oscillations are increased significantly. The amplitude of the steady-state oscillations is also increased to a higher value with an average value of 0.77 radians (about 44.12°).

Fig.4 shows the effect of the corresponding difference of the angular velocities for stiffness coefficients, K=450Nm/rad, K=297Nm/rad and K=45Nm/rad, respectively. Close observation theses waveforms show that unlike the difference between angles, the speed difference at the both ends of the shaft increases and decreases again as K is reduced, which means that there is a certain K which makes the speed difference

maximum. Also we observe that the speed from the motor side might be higher or lower than the value of the speed from load side until the difference vanishes. At the steady-state operation, the average value of the speed difference will be almost zero. In case of more flexible shaft, the amplitude of the oscillations of the speed difference drops to very small values at steady-state operation.

The value of the stiffness coefficient K is affected by the shaft dimensions i.e. the length (L_{shaft}) and the diameter (D_{shaft}). Thus as the value of K is decreased, then this means that the shaft diameter (D_{shaft}) is decreased or the shaft length (L_{shaft}) is increased or the modulus of elasticity is decreased. Decreasing the shaft diameter will result in reduction of the cost of the shaft, which is considered as an advantage.

For the same Young's modulus of the shaft material, the stiffness coefficient K variation is achieved through the change of the shaft dimensions. For instance, for K=450Nm/rad, the shaft diameter is 3 cm and the shaft length is calculated as 9 cm for a shaft's material of Young's modulus, E=1.38GPa and Poisson's ratio (v) of 0.32. But for the same material and same shaft diameter, for a stiffness coefficient K=297Nm/rad the shaft length is calculated as 14cm, and for the stiffness coefficient of K=45Nm/rad, the shaft's length is found to be 70cm. Therefore as the stiffness coefficient K reases for the same material and same diameter, the shaft length (L_{shaft}) increases. In this case, the diameters of the shaft of a constant length of 70cm will be 5cm, 4.5cm and 3cm for K=450Nm/rad, K=297Nm/rad and K=45Nm/rad, respectively for a shaft of the same Young's modulus. Therefore, whenever the cost of the system is important it is recommendable to use relatively longer shaft with smaller diameter, as long as the shaft will not face shaft fatigue and deflection for a given maximum load torque.

The effect of stiffness coefficient on the dc link current of the drive are depicted in Figs.5.a, 5.b and 5.c for stiffness coefficients of K=450Nm/rad, K=297Nm/rad and K=45Nm/rad, respectively.

From observation of these figures it becomes evident that as the shaft becom more flexible, i.e. K decreases, the transient peaks of the dc link current decreases a they converge to the same steady-state amplitude whereas the transient time duration is prolonged.

The effect of the stiffness coefficient on the load torque is shown in Fig.6. Since the load torque is a function of the angular speed from the load side, than the shapes of load torque and ω_{r2} with respect to time will be similar. This fact is clearly seen from Figs.6.a, 6.b and 6.c, which are obtained for a rigid shaft, K=297Nm/rad and K=45Nm/rad, respectively. The load torque is having larger oscillation around the average torque. It increases up to a certain value of K and then decreases again as the shaft becomes more flexible.

The effect of the degree of shaft stiffness coefficient on the electromagnetic torque is shown in Figs.7.a, 7.b and 7.c for rigid shaft and K=297Nm/rad and K=45Nm/rad, respectively. Observation of these figures shows that as the shaft becomes more flexible the peaks of the electromagnetic torque oscillations show minor reduction. Therefore, shaft flexibility has negligible effect on the electromagnetic torque. Therefore, from electromagnetic torque point of view, shaft can be as flexible as it is convenient.

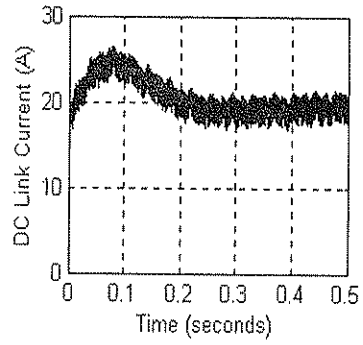

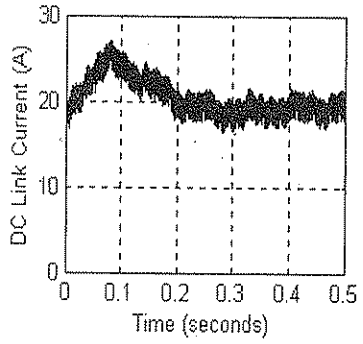

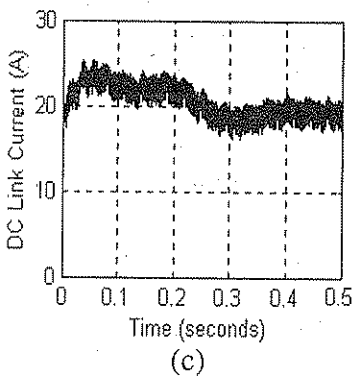

Figure 5. DC link current.
(a) K=450 (b) K=297 (c) K=45

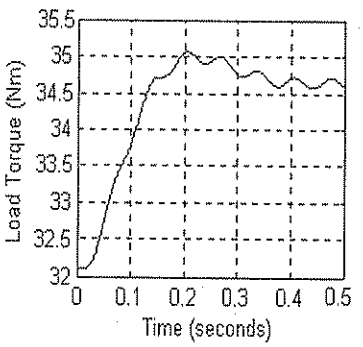

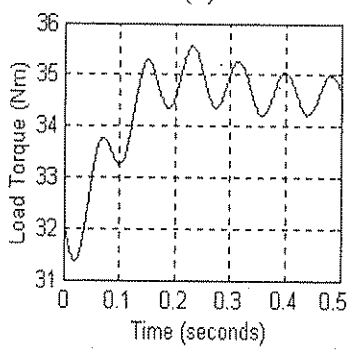

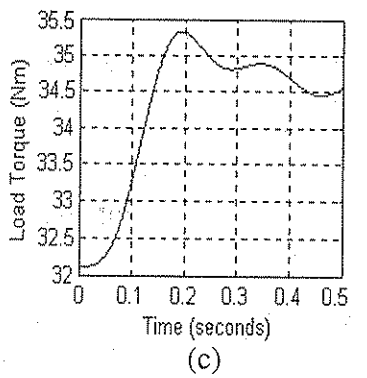

Figure 6. Load torque.
(a) K=450 (b) K=297 (c) K=45

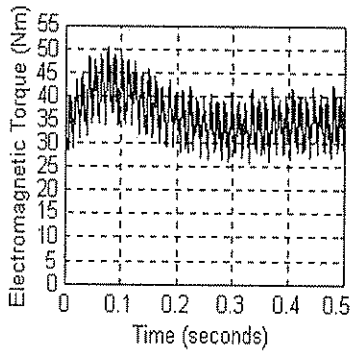

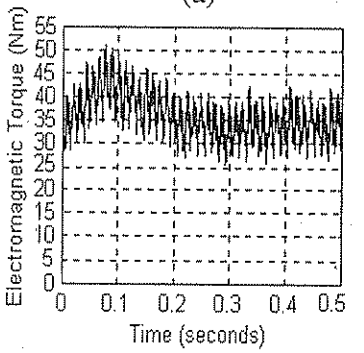

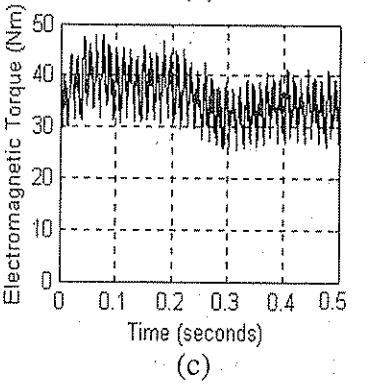

Figure 7. Electromagnetic torque.
(a) K=450 (b) K=297 (c) K=45

5. CONCLUSIONS

In this paper a mathematical model is developed to study the effect of shaft flexibility on the performance of SERD and the performance of the drive is studied in details, for various values of the shaft stiffness coefficient. This study provides useful guidelines for designers of induction motors for SERD applications. It is proposed that two options are available for designers:

- Reduced cost
- Faster transient response

If the reduced cost is taken as the design target, more flexible shafts, made of such materials as composites or polymers, with reduced shaft diameter should be used. These types of shafts are preferred in certain applications such as submarines. In this case the performance of the drive will have the following characteristics:

- Prolonged transient time duration, which might increase the temperature rise of the windings during starting
- Larger differences between the speeds and the angles at the two ends of the shaft during transient state. At a certain K the speed difference passes through a maximum and than tends to decrease again.
- Larger oscillations and overshoot of the load torque
- Reduced electromagnetic torque peaks during both the transient period and the steady-state operation
- Higher amplitude and lower frequency speed oscillations during the transient period
- Reduced dc link current oscillations.

On the other hand if the faster transient response is chosen as the design target, then rigid shafts should be preferred, which will show opposite operating characteristic to that of the flexible shafts.

REFERENCES

[1] Craig, Roy R., Jr., *Mechanics of Materials,* John Wiley & Sons, USA, 1996.

[2] Hall, Jr., A.S., Hollowenko, A.R. and Laughin, H.G., *Schaum's outline of Theory and Properties of Machine Design*, McGraw Hill Book Company, USA, 1961.

[3] Personal Communication with TECO- Westinghouse Motor Company.

[4] Deur, J. and Peric, N., Analysis of Speed Control System for Electrical Drives with Elastic Transmission, *ISIE'99-Bled, Slovenia, 1999 IEEE*, pp. 624-630.

[5] Schroder, D., Requirements in Motion Control Applications, invited paper at *1992 IFAC Workshop* on Motion Control for Intelligent Automation.

[6] Lindfield, G. and Penny, J., *Numerical Methods Using MATLAB*, Ellis Horwood, USA, 1995.

[7] Akpinar, E. and Pillay, P., Modeling and Performance of Slip Energy Recovery Induction Drives, *IEEE Trans. on Energy Conversion*, Vol. 5, No. 1, March 1990, pp. 203-210.

[8] Akpinar, E. and Pillay, P., A Computer Program to Predict the Performance of Slip Energy Recovery Induction Drives, *IEEE Trans. on Energy Conversion*, Vol. 5, No. 2, June1990, pp.357-365.

[9] Weinstock, R., *Calculus of Variations with Applications to Physics and Engineering, Dover Publishings*, INC., USA, 1974.

[10] Hass, W., Schlacher, K. and Gahleitner, R., Modeling of Electromechanical Systems, *Master thesis*, Johannes Kepler University Linz, 2000.

[11] Charles, J.A. and Crane, F.A. A., *Selection and Use of Engineering Materials*, Butterworth Heinemann Ltd., Great Britain,1989.